Optics Letters

Multioctave and reconfigurable frequency-stepped radar waveform generation based on an optical frequency shifting loop

YAMEI ZHANG, CE LIU, KUNLIN SHAO, ZHAOYU LI, AND SHILONG PAN*

Key Laboratory of Radar Imaging and Microwave Photonics, Ministry of Education, Nanjing University of Aeronautics and Astronautics, Nanjing 210016, China
*Corresponding author: pans@nuaa.edu.cn

Received 20 January 2020; revised 16 February 2020; accepted 17 February 2020; posted 20 February 2020 (Doc. ID 388743); published 30 March 2020

A photonic method for multioctave and reconfigurable frequency-stepped radar waveform generation is proposed and experimentally demonstrated based on an optical frequency shifting loop (OFSL). When a rectangular optical pulse is applied to the OFSL, a frequency-stepped optical signal can be generated. Beating the signal with another continuous-wave optical carrier, an electrical frequency-stepped waveform can be obtained. By meticulously adjusting the relations between the time duration of the rectangular optical pulse and the loop delay of the OFSL, the frequency-hopping rate (or the frequency-hopping period) of the generated frequency-stepped signal can be reconfigured. An experiment is carried out. The generation of frequency-stepped signals with frequency intervals of 1 GHz, 3 GHz, 5 GHz, 8 GHz, and 10 GHz is realized. The reconfigurability of the frequency-hopping period is also investigated and different frequency-hopping periods of 189, 10.2, 5.1, and 2.42 ns are achieved.

https://doi.org/10.1364/OL.388743

Frequency-stepped waveforms with reconfigurable frequency, fast frequency-hopping speed, and a large time-bandwidth product (TBWP) are widely used in radar, communications, and electronic warfare systems thanks to the advantages in terms of broad detection range, high-range resolution, excellent anti-interference capability, and low signal processing complexity [1,2]. Conventionally, frequency-stepped signals are generated with pure electronic technologies, which suffer severely from the limited bandwidth and low central frequency. To deal with these problems, photonics-based frequency-stepped waveform generation methods have been proposed due to the intrinsic characteristics of photonic technologies, such as high frequency, broad bandwidth, low transmission loss, and electromagnetic interference immunity [3–5]. Tremendous efforts have been devoted to generating frequency-stepped waveforms, which are mainly divided into two categories, i.e., spectra shaping and frequency to time mapping (FTTM) [6,7], and the optical heterodyning method [8–18].

The FTTM-based method is implemented by manipulating the ultra-broadband spectra of an ultra-narrow optical pulse according to the shape of a frequency-stepped waveform and then mapping the spectra into the time domain via a dispersive element. This method features a large operational bandwidth, high central frequency, and excellent flexibility, but the generated signal has a limited time duration (around 10 ns) and poor spectrum purity.

The optical heterodyning method is generally realized by generating a frequency-stepped optical signal and beating it with an optical carrier or another frequency-stepped optical signal at a photodetector (PD). The key is the generation of the frequency-stepped optical signal. In Refs. [8,9], a semiconductor laser source that externally injected by an electrical-waveform modulated optical signal is adopted. This system can generate signals within a broad frequency range and a large time duration. However, limited by the maximum tolerable voltage of the period-one oscillation, the maximum bandwidth of the generated signal is limited to ~ 15 GHz. In Ref. [12], an optical frequency comb generator (OFC) incorporated with a silicon microring resonator (MRR) is employed to produce the frequency-stepped signal. The key of this approach is to select different comb lines by thermally tuning the MRR, leading to a very slow frequency switching time (about hundreds of microseconds) in the generated signal. In Ref. [14], a frequency-sweeping laser source is employed to generate a frequency-stepped signal. The bandwidth and time duration could be very large; however, the beating of two uncorrelated laser sources would worsen the stability and the spectra purity of the generated signal.

The frequency-stepped signal can also be obtained by photonic microwave frequency multiplying based on the electro-optic nonlinear effect [16,17,19,20]. However, it is quite challenging to generate a multioctave frequency-stepped signal due to the relatively severe harmonic crosstalk.

In this Letter, we propose and experimentally demonstrate a multioctave frequency-stepped signal generator based on an optical frequency shifting loop (OFSL). The system features a broad operation bandwidth (larger than 26 GHz) and flexible

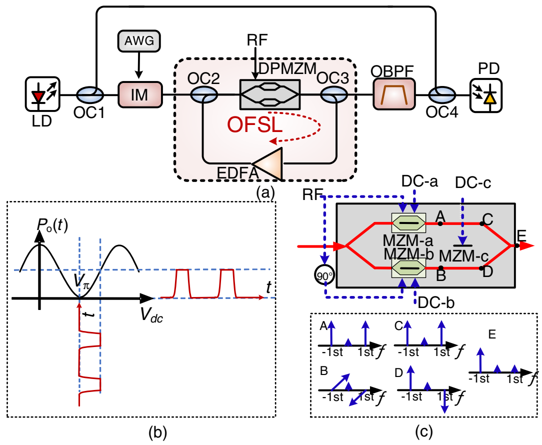

Fig. 1. (a) Schematic diagram of the frequency-stepped signal generator. Illustrations of (b) the principle of the IM and (c) the spectra evolutions in the DPMZM.

frequency-hopping period reconfigurability. Signals with reconfigurable frequency-hopping periods and symbols of frequency intervals can be obtained.

Figure 1(a) shows the schematic diagram of the proposed frequency-stepped signal generator. A continuous-wave light from a laser diode (LD) is split into two branches. An intensity modulator (IM), an OFSL, and an optical bandpass filter (OBPF) are inserted into one branch. The two branches are then combined. The IM is driven by an electrical rectangular pulse train, which is employed to perform the optical switch (OS) function as shown in Fig. 1(b). Supposing the expression of the optical carrier applied to the OS is $E_{\rm in}(t) = \cos(\omega_o t)$, where ω_o is the angular frequency of the optical carrier, the output of the OS can be written as

$$E_{\rm OS}(t) = \sum_n \mathrm{rect}\left[\frac{t - nT_s - \tau/2}{\tau}\right] \cos(\omega_o t), \tag{1}$$

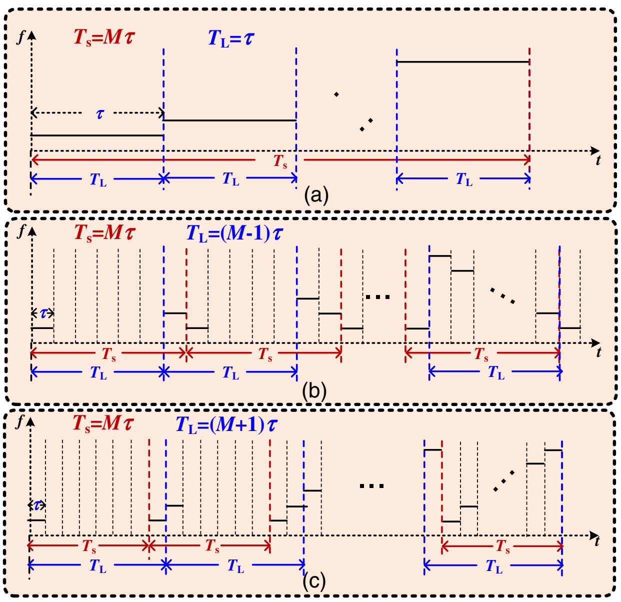

Fig. 2. Illustrations of the frequency evolutions. (a) Slow frequency-stepped signal in Eq. (2), (b) fast frequency-stepped signal with descending frequencies in Eq. (3), and (c) fast frequency-stepped signal with ascending frequencies in Eq. (4).

where τ and T_s are the pulse width and the period of the rectangular pulses is $T_s = M\tau$ (M is an integer). From Eq. (1) we can see that the optical switching function is realized and a rectangular optical pulse is generated, which is then injected into the OFSL. The OFSL consists of a frequency shifter, an optical amplifier, and two optical couplers (OCs). The frequency shifter is realized by a dual-parallel Mach–Zehnder modulator (DPMZM) that is driven by a pair of quadrature RF signals with an angular frequency of ω_s as shown in the upper portion of Fig. 1(c), and the spectra evolution in the DPMZM is shown in the lower portion of Fig. 1(c).

The frequency-shifted signal is then split into two paths; one is straight back to the frequency shifter and undergoing another frequency-shifting circulation and the other is output from the OFSL. When the loop delay T_L of the OFSL is equal to the pulse width of the rectangular optical pulse, i.e., $T_L = \tau$, there would be only one frequency component output by the DPMZM during T_L period (as shown in Fig. 2(a)) and the output of the OFSL can be expressed as

$$E_{\rm OFSL}(t) = \sum_n \left\{ \mathrm{rect}\left[\frac{t - nT_s - T_s/2}{T_s}\right] \cdot \sum_{m=0}^{M} \mathrm{rect}\left[\frac{t - m\tau - \tau/2 - nT_s}{\tau}\right] \cos\{[\omega_o + (m-1)\,\omega_s]\,t\} \right\}. \tag{2}$$

Equation (2) represents a frequency-stepped optical signal, and the frequency-hopping period is equal to T_L.

If τ is adjusted to let $T_L = (M-1)\tau$ as depicted in Fig. 2(b), Eq. (2) would be changed to

$$E_{\rm OFSL}(t) = \sum_n \left\{ \mathrm{rect}\left[\frac{t - nT_s - T_s/2 - (M-1)\,T_L}{T_s}\right] \cdot \sum_{m=0}^{M-1} \mathrm{rect}\left[\frac{t - m\tau - \tau/2 - nT_s - (M-1)\,T_L}{\tau}\right] \times \cos\{[\omega_o + (M-m-1)\omega_s]\,t\} \right\}. \tag{3}$$

Equation (3) denotes a frequency-stepped optical signal with a frequency interval of $-\omega_s$, and the frequency-hopping period equals $T_L/(M-1)$.

If τ is adjusted to let $T_L = (M+1)\tau$ as illustrated in Fig. 2(c), Eq. (2) would become

$$E_{\rm OFSL}(t) = \sum_n \left\{ \mathrm{rect}\left[\frac{t - T_s/2 - (n+M-1)\,T_s}{T_s}\right] \cdot \sum_{m=0}^{M-1} \mathrm{rect}\left[\frac{t - m\tau - \tau/2 - (n+M-1)\,T_s}{\tau}\right] \times \cos\{[\omega_o + m\omega_s]\,t\} \right\}. \tag{4}$$

Equation (4) shows a frequency-stepped optical signal with a frequency interval of ω_s, and the frequency-hopping period equals $T_L/(M+1)$.

Combining the signal in Eqs. (2), (3), or (4) with the optical carrier from the other branch, and sending them into a PD, an electrical frequency-stepped signal can be generated. If the repetition period of the pulsed optical carrier is large enough, a multioctave frequency-stepped signal from DC to the maximum frequency of the PD can be generated. It should be noted that arbitrary frequency-coding cannot be realized with this structure and the circulation of the optical signal in the OFSL would worsen its coherence with the optical carrier from the upper path, so the phase noise may be affected.

A proof-of-concept experiment is carried out based on the setup shown in Fig. 1. A lightwave with a wavelength of 1550.45 nm and a power of 14 dBm is generated by a LD and is split into two branches via a 50:50 OC (OC1). The lightwave in one branch is sent to an OS to obtain a rectangular optical pulse. The OS is performed by an IM with an extinction ratio of 20 dB, a 3-dB bandwidth of 25 GHz, and a half-wave voltage of 2.8 V, and is controlled by an electrical rectangular pulse train generated by an arbitrary waveform generator (AWG). After the OS, the rectangular optical pulse is applied to the OFSL, which consists of a DPMZM, an erbium-doped fiber amplifier (EDFA), and two OCs (OC2 and OC3). The DPMZM has a 3-dB bandwidth of 22 GHz and a half-wave voltage of 3.5 V, and it is driven by an RF signal generated by a signal generator (Agilent 8257D). The loop length of the OFSL is around 37.8 m, corresponding to a loop delay of 189 ns. At the output of the OFSL, the frequency-stepped optical signal can be generated. An OBPF is then followed to remove the out-of-band noises and sidebands. After filtering, the signal is combined with the signal from the other branch. The combined signals are then beating at a PD with a 3-dB bandwidth of 30 GHz and a responsivity of 0.65 A/W. Polarization controllers with a polarization extinction ratio of 20 dB are inserted after the LD and in the OFSL to match the polarization states of the signal. The electrical waveforms are observed by a 32-GHz real-time oscilloscope.

Figure 3(a) shows the optical spectrum obtained at the output of the OBPF when the OFSL loop is open, and the frequency of the RF signal applied to the OFSL is 5 GHz. As can be seen, carrier suppressed single-sideband (CS-SSB) modulation is realized, in which, the optical carrier is 22 dB smaller than the remaining first-order sideband, indicating that frequency shifting is implemented. Then, the OFSL is closed and the spectrum at the output of the OBPF is shown in Fig. 3(b). More than 15 comb lines are observed in Fig. 3(b). The power variation is smaller than 2 dB for most of the comb lines. The fast falling of the optical power is introduced by the OBPF followed by the OFSL. The 3-dB bandwidth of the OBPF is about 0.65 nm. The frequency interval depends on the RF frequency applied to the OFSL, and the frequency-hopping period depends on the open time of the OS.

The frequency-stepped optical signal is then combined with the optical signal from the other branch and beaten at a PD. Figures 4(a) and 4(b) show the measured waveform of the generated frequency-stepping signal and the recovered instantaneous frequency. As can be seen, the frequency of the generated signal is stepped from 5 to 30 GHz with an interval of 5 GHz over a time duration of 1.2 μs. The amplitude jumps between adjacent frequency components are due to an uneven optical frequency-stepped signal shown in Fig. 3(b) and the uneven response of the PD. The frequency-hopping period is ∼ 200 ns, which is a

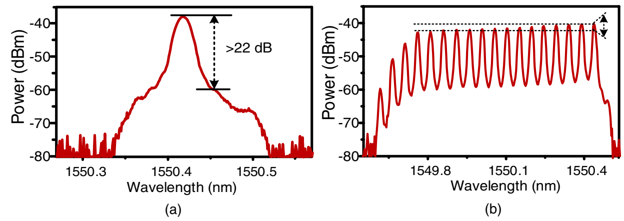

Fig. 3. Optical spectra of the CS-SSB modulated signal at the output of the OBPF when the OFSL is (a) open and (b) closed. The frequency of the signal applied to the OFSL is 5 GHz.

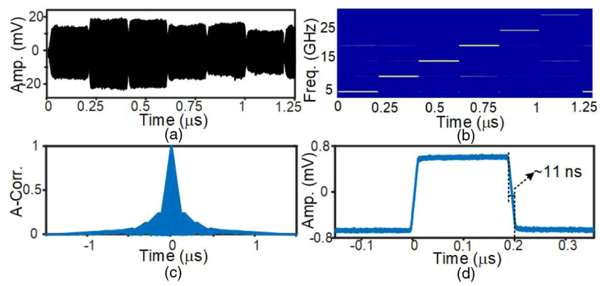

Fig. 4. (a) Waveform, (b) the instantaneous frequency, and (c) the autocorrelation function of the generated signal with a frequency interval of 5 GHz, and (d) the waveform of the electrical rectangular pulse.

bit larger than the pre-set value 189 ns. The difference is mainly due to the relatively slow edges of the electrical rectangular pulse as shown in Fig. 4(d). The mismatch of the loop delay and the pulse width would worsen the frequency purity of the generated signal. Figure 4(c) shows the autocorrelation function of the generated signal, and the full width at half-maximum (FWHM) of the compressed pulse is about 200.6 ns, agreeing well with the theoretical result of 200 ns. The pulse compression ratio (PCR) is calculated to be 5.98 as the pulse width before compression is around 1.2 μs.

To evaluate the frequency tunability of the proposed system, the frequency of the RF signal is changed to be 1 GHz and the results are illustrated in Fig. 5. A frequency-stepped signal with frequency stepping from 4 to 30 GHz is observed. The time duration of the signal from 4 to 30 GHz is about 5 μs, and the FWHM of the autocorrelated pulse is about 224 ns, corresponding to a PCR of ∼ 22.3. Then the frequency is changed to be 3, 8, and 10 GHz, and the repetition rate of the rectangular pulse is also changed to avoid signal overlapping. The results are depicted in Figs. 5(c)–5(h). The frequency ranges of the three conditions are from 3 to 30, 8 to 32, and 10 to 30 GHz, and the time durations are about 2.1, 0.84, and 0.6 μs. The FWHMs of the autocorrelated pulses are 219, 220, and 214 ns, corresponding to PCRs of 9.6, 3.8, and 2.8. Mainly due to the poor harmonics suppression, the PCRs are smaller than the theoretical results of 10, 4, and 3. If a DPMZM with a higher extinction ratio is employed in the OFSL, the residual harmonic components can be efficiently suppressed and the PCR can be optimized.

It should be noted that the FWHM is limited to the frequency-hopping period (around 200 ns), which is equal to the loop delay of the OFSL. Since the OFSL is realized by discrete devices, with a total length of about 37.8 m, a large

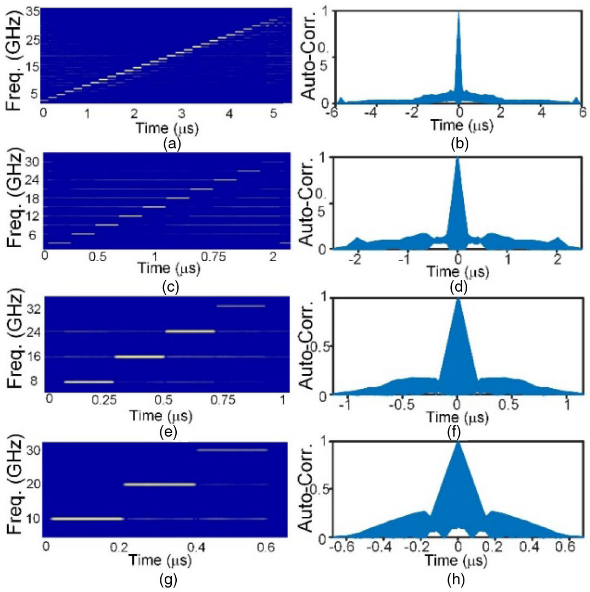

Fig. 5. Instantaneous frequency and the autocorrelation functions of the generated frequency-stepped signals with frequency intervals of (a), (b) 1 GHz, (c), (d) 3 GHz, (e), (f) 8 GHz, and (g), (h) 10 GHz.

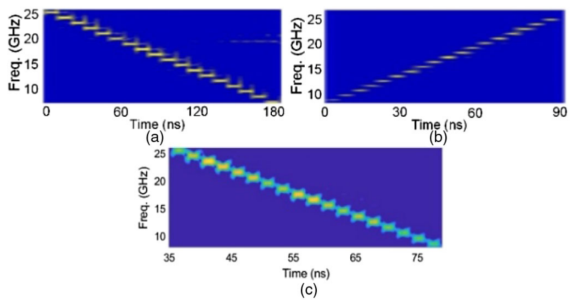

Fig. 6. Instantaneous frequency of the fast frequency-stepped signal with frequency-hopping periods of (a) 10.2 ns, (b) 5.1 ns, and (c) 2.42 ns.

frequency-hopping period and a low frequency-hopping rate result. To deal with this problem, the pulse width of the rectangular optical pulse is changed according to Eqs. (3) and (4) and electrical pulses with pulse widths of 10 ns ($M = 20$), 5 ns ($M = 37$), and 2.5 ns ($M = 77$) are employed as the driven signal of the OS.

Figure 6 shows the instantaneous frequencies of the three generated frequency-stepped signals. The frequencies are over 8 to 25 GHz with an interval of -1 GHz ((a) and (c)) or 1 GHz (b). The frequency-hopping periods of Figs. 6(a)–6(c) are about 10.2 ns, 5.1 ns, and 2.42 ns, agreeing well with the theoretical values of 10, 5, and 2.5 ns, indicating that fast frequency-stepped signals with different frequency-hopping periods and different symbols are generated.

In conclusion, a multioctave and reconfigurable frequency-stepped waveform generator based on an OFSL was proposed and experimentally demonstrated. The multioctave frequency range was realized with multiple frequency shifting of a relatively low-frequency-driven signal in the OFSL, and the reconfigurability is achieved by adjusting the relations between the pulse width of the rectangular optical pulse and the loop delay of the OFSL. Fast frequency-stepped signals with descending and ascending frequencies were produced; the frequency-hopping period can be as small as 2.42 ns. The method can be extended to realize multiband linearly or nonlinearly frequency modulated signal generation [21–23], which could find potential applications in a broadband radar system to improve the range detection resolution and the anti-interference capability.

Funding. National Key Research and Development Program of China (2018YFB2201803); National Natural Science Foundation of China (61901215); Jiangsu Provincial “333” Project (BRA2018042); Fundamental Research Funds for the Central Universities; Natural Science Foundation of Jiangsu Province (BK20190404).

Disclosures. The authors declare no conflicts of interest.

REFERENCES

1. M. Skolnik, *Radar Handbook*, 3rd ed. (McGraw-Hill, 2008).
2. M. K. Simon, *Spread Spectrum Communications Handbook* (McGraw-Hill, 1994).
3. J. Capmany and D. Novak, Nat. Photonics **1**, 319 (2007).
4. J. Yao, J. Lightwave Technol. **27**, 314 (2009).
5. S. L. Pan, D. Zhu, and F. Z. Zhang, Trans. Nanjing Univ. Aeronaut. Astronaut. **31**, 219 (2014).
6. A. Rashidinejad and A. M. Weiner, J. Lightwave Technol. **32**, 3383 (2014).
7. C. Wang and J. P. Yao, J. Lightwave Technol. **28**, 1652 (2010).
8. P. Zhou, F. Z. Zhang, Q. S. Guo, S. Li, and S. L. Pan, IEEE J. Sel. Top. Quantum Electron. **23**, 1801109 (2017).
9. P. Zhou, F. Z. Zhang, X. W. Ye, Q. S. Guo, and S. L. Pan, IEEE Photon. J. **8**, 5501909 (2016).
10. T. F. Hao, Q. Z. Cen, Y. T. Dai, J. Tang, W. Li, J. P. Yao, N. H. Zhu, and M. Li, Nat. Commun. **9**, 1839 (2018).
11. O. L. Coutinho, J. Zhang, and J. Yao, in *International Topical Meeting on Microwave Photonics, Paphos, Cyprus* (2015), p. 1.
12. F. Zhou, X. Wang, S. Q. Yan, X. Hu, Y. G. Zhang, H. Q. Qiu, X. Xiao, J. J. Dong, and X. L. Zhang, IEEE Photon. J. **10**, 7800809 (2018).
13. X. Feng, L. S. Yan, H. Y. Jiang, P. Li, J. Ye, Y. Zhou, W. Pan, B. Luo, X. H. Zou, and T. Zhou, IEEE Photon. J. **11**, 5500207 (2019).
14. J. W. Shi, F. M. Kuo, N. W. Chen, S. Y. Set, C. B. Huang, and J. E. Bowers, IEEE Photon. J. **4**, 215 (2012).
15. Y. Chen, IEEE Photon. J. **10**, 5500407 (2018).
16. Q. S. Guo, F. Z. Zhang, P. Zhou, and S. L. Pan, IEEE Photon. Technol. Lett. **29**, 1320 (2017).
17. K. Zhang, S. H. Zhao, X. Li, Z. H. Zhu, W. Jiang, T. Lin, and G. D. Wang, Opt. Commun. **437**, 17 (2019).
18. Y. M. Zhang and S. L. Pan, IEEE J. Quantum Electron. **54**, 0700112 (2018).
19. F. Z. Zhang, Q. S. Guo, Z. Q. Wang, P. Zhou, G. Q. Zhang, J. Sun, and S. L. Pan, Opt. Express **25**, 16274 (2017).
20. X. W. Ye, F. Z. Zhang, Y. Yang, and S. L. Pan, Photon. Res. **7**, 265 (2019).
21. H. G. D. Castellus, in *Optical Fiber Communications Conference (OFC)*, OSA Technical Digest (Optical Society of America, 2019), paper Th3C.1.
22. L. Herrera, R. Ribeiro, V. Jabulka, P. Tovar, and J. Weid, J. Lightwave Technol. **36**, 4408 (2018).
23. P. Tovar, L. Herrera, R. M. Ribeiro, and J. Weid, IEEE Photon. Technol. Lett. **31**, 1417 (2019).